ACS APPLIED MATERIALS & INTERFACES

Research Article

www.acsami.org

Room-Temperature Humidity-Sensing Performance of SiC Nanopaper

Gong-yi Li,* Jun Ma, Gang Peng, Wei Chen, Zeng-yong Chu, Yi-he Li, Tian-jiao Hu, and Xiao-dong Li

College of Science, National University of Defense Technology, Changsha, People's Republic of China, 410073

Supporting Information

ABSTRACT: Centimeters-long SiC nanowire could be a strong "bridge" between microworld and macroworld due to its unique morphology, excellent chemical stability, and intriguing physical properties. Here we present a novel "paperlike" material—free-standing SiC nanopaper fabricated by acetone-assisted compression of centimeters-long SiC nanowires. The resistance of this new paperlike material linearly increases with increasing environmental relative humidity in a very short time. We suggest that adsorption of water molecules on SiC nanopaper surface led to fast electron transfer between SiC nanopaper and water layer, which indicates that SiC nanopaper could be applied to high-performance humidity sensor in harsh environment.

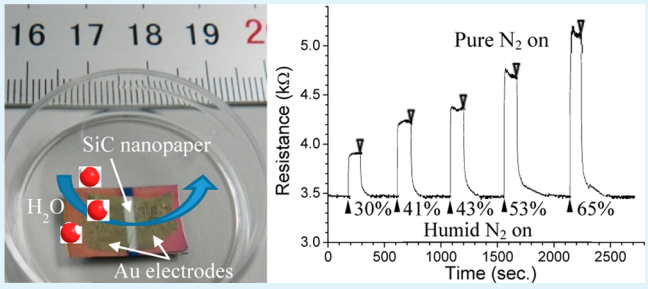

KEYWORDS: *SiC nanowires, nanopaper, humidity sensor, sensing mechanism*

INTRODUCTION

The electrical conductivity of nanomaterials could be changed in the presence of water vapor. Four well-documented mechanisms including (1) ionic conduction based on dissociative adsorption of water molecules;[1] (2) depletion-layer variation resulting from competitive water physisorption;[2] (3) electron transfer induced by weak interaction between water molecules and nanomaterials;[3,4] and (4) change in the tunneling distance[5] were proposed to explain their resistance variation. Compared with bulk materials, nanomaterials as humidity-sensing element has shown improved sensing performance[1] owing to the special chemical and physical properties and high specific surface area derived from reduced sizes. On the basis of the above mechanisms, Al_2O_3 nanotubes,[6] ZnO nanomaterials,[1,7] CeO_2 nanowires,[8] $Na_3Ti_3O_7$ nanowires,[9] SnO_2 nanowires,[2] CNT,[4,10] and graphene quantum dots[5] have been successfully utilized to detect the environmental relative humidity (RH) to serve potential applications such as water-sensitive chemical and microelectrical industrial processes as well as our living environment.[11,12] Even for gas sensor, humidity control is also an important factor to get better sensing performance.[13] However, humidity sensors based on metal oxides and CNT may have many challenges while being applied in hostile environment containing corrosive and hazardous chemicals. To prepare robust sensing materials of high-performance is still a challenge, especially in troubles of increasingly serious environmental pollution including acid rain.

"Paperlike" materials based on nanomaterials including buckypaper,[14−17] graphene paper,[18] graphene oxide paper,[19] and other inorganic paper[20] have been extensively studied for their potential applications from reinforcements to functional materials. Recently, studies of composite paper containing CNT, graphene, and graphene oxide also show potential applications in energy-storage devices,[21] high-performance flexible electrodes,[22] and visual bioassays.[23] Because of the nature of SiC materials,[24] SiC nanomaterials are excellent functional materials that could be potentially utilized in harsh environment including acid/alkaline environment and oxidizing atmosphere at high temperature. Here we report a novel paperlike material—free-standing SiC nanopaper. It was fabricated by acetone-assisted compression of randomly aligned centimeters-long SiC nanowires, showing good humidity-sensing properties at room temperature. As the first study of humidity-sensing property of resistive-type device based on SiC nanomaterial, an intriguing phenomenon that effective carrier density of SiC nanopaper linearly decreases with increasing humidity was discovered and tentatively discussed.

RESULTS AND DISCUSSION

Free-standing SiC nanopaper was fabricated via precursor pyrolysis chemical vapor deposition (PPCVD) route[25] and acetone-assisted compression method in turn. Generally, SiC nanopaper is a thin film made of a large number of compressed SiC nanowires. Detailed information on preparation and characterization of centimeters-long SiC nanowires is available in our previous paper.[25] Figure 1 demonstrates a flat piece of SiC nanopaper, and SiC nanowires can be clearly seen in the enlarged image (Figure 1b). As shown in Supporting Information, Figure S1, centimeters-long SiC nanowires were first placed on a silicon wafer (which could also be weighing

Received: October 3, 2014
Accepted: December 3, 2014
Published: December 3, 2014

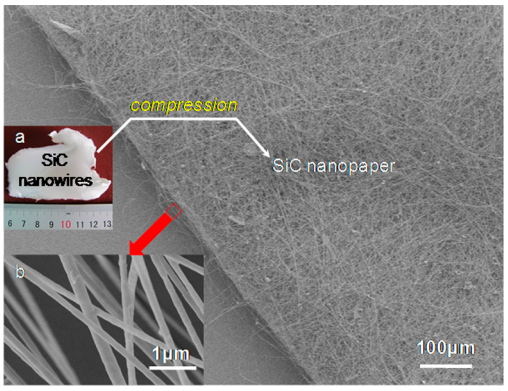

Figure 1. SEM images and photographs (a) of SiC nanopaper (inset b is the enlarged image of rectangular area).

paper or other substrates that SiC nanopaper could be easily peeled off), then several drops of acetone were dropped on the sample and allowed to volatilize naturally at room temperature. The cotton-like centimeters-long SiC nanowires were compressed to a piece of SiC nanopaper during the process. The thickness of SiC nanopaper depends on the quantity of nanowires for compression process. And the SiC nanopaper could be easily tailored by scissor to the desired size like a normal paper. (Photos of tailoring SiC nanopaper are available in Figure S1.)

SiC nanopaper or SiC nanowires are electrically conductive as shown in Figure 2. To be used in practical electronic device, the electrical properties of SiC nanopaper were measured by digital multimeter (Agilent 34411A) before and after sputtering Au electrode with thickness of ~0.5 μm. The darker region of SiC nanopaper (lower right of Figure 2a) is the part without electrode, which could be easily observed by SEM at low magnification. Their current versus voltage (I–V) curves are shown in Figure 2a, and the resistance of the SiC nanopaper (size: 12 mm × 7 mm × 10 μm) decreased from 21.14 kΩ to 2.82 kΩ after sputtering Au electrode with an alumina foil mask (1.5 mm in width). The resistance change was reasonable because the part of SiC nanopaper covered by Au electrodes became a perfect conductor. And the larger area covered by Au electrode of SiC nanopaper, the lower resistance of SiC nanopaper we obtained. The straight I–V curve of the SiC nanopaper with Au electrode also indicates good contact between SiC nanopaper and testing circuit. According to the equation $\rho = RS/L$ (ρ is resistivity, R is resistance, L is the length of SiC nanopaper, and S is the maximum cross-sectional area when SiC nanowires with average diameter of 150 nm are close packed), the calculated maximum resistivity of the SiC nanopaper and the sputtered SiC nanopaper is 12.9 and 13.8 Ω·cm, respectively. The calculated resistivity is comparable with that of a single SiC nanowire field effect transistor (SiC FET) as indicated by Figure S2 (14.63 and 1.10 Ω·cm at drain-source voltage of 0.1 and 3 V, while gate voltage (V_g) is 0 V), and also with that of the single SiC nanowire (5.8 Ω·cm) in Chen's work.[26]

To find out the main carrier type in the SiC nanopaper, a FET based on single SiC nanowire was fabricated by electron beam lithography method, as shown in Figure 2b and Figure S2. The drain current (I_d) was measured by Keithley 4200-SCS. Figure 2b is the curve of I_d versus V_g. As can be seen, I_d decreases when V_g varied from −80 to 80 V, which confirms the p-type channel of the SiC nanowire.[26] In contrast to the documented SiC one-dimensional nanostructures of n-type semiconductor,[27,28] the p-type SiC nanowires in our work may be caused by the silane fragment from the decomposition of liquid polysilacarbosilane during the preparation. The ratio of Si and C in the silane fragment was usually not 1:1, and thus it could form some vacancy in the final crystal SiC nanowires.

Adsorption of water molecules on the solid surface of some nanomaterials, such as ZnO,[1] SnO_2,[2] and CNT,[4] usually changes the conductivity of the nanostructures. We also observed certain influences of the water vapor on the electrical resistance of SiC nanopaper in the experiment. To fully understand the humidity-sensing performance and demonstrate the potential application of SiC nanopaper, resistive-type sensor of SiC nanopaper was prepared (similar to the device shown in Figure 2a) to test the resistance variation of SiC nanopaper sensor in humid atmosphere. Three methods (**I**, **II**, and **III**) were applied to adjust the RH of testing system (details of the three methods are described in the Methods Section, and the schematic illustrations of testing systems are shown in Figure S2).

The typical humidity response of SiC nanopaper examined by method **I** in humid atmosphere is shown in Figure 3a. The resistance of SiC nanopaper rapidly increased and gradually reached a plateau when exposed to humid nitrogen. According to eq 1, the response to humidity of SiC nanopaper could reach as high as 47.43% (RH = 65%), while the R_0 is the resistance of the sensor in the absence of analyte and ΔR is the resistance

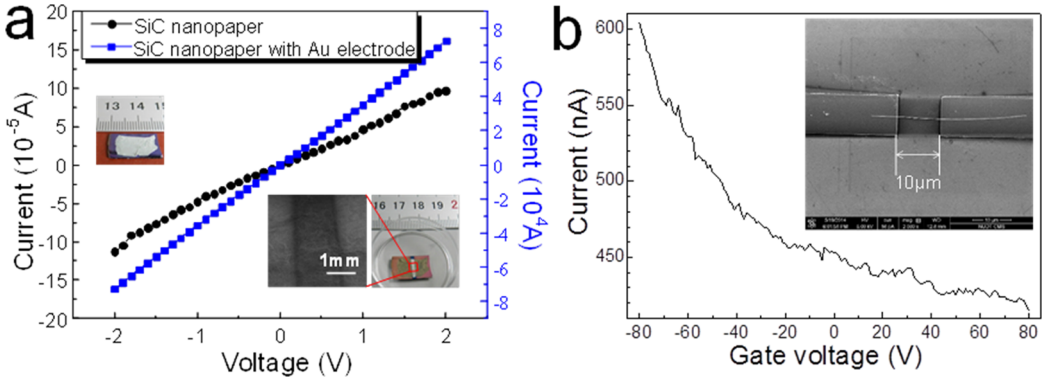

Figure 2. (a) Current vs voltage curves of the SiC nanopaper before and after sputtering Au electrode; the insets are the photos of SiC nanopaper with and without Au electrode; (b) The drain current vs gate voltage curve obtained at the drain-source voltage of 3 V, and the inset is the SEM image of the single SiC nanowire FET prepared by electron beam lithography method.

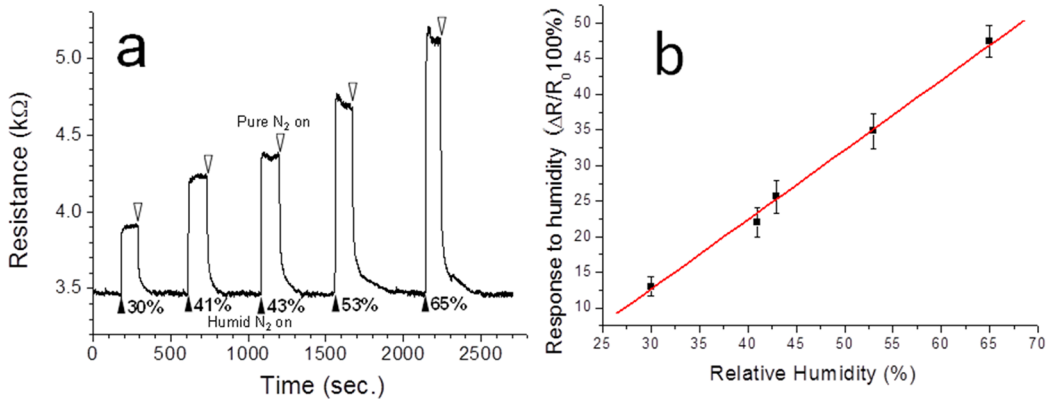

Figure 3. (a) The humidity-sensing performance of SiC nanopaper in the atmosphere of different RH (30%, 41%, 43%, 53% and 65%) at 15 ± 0.3 °C (up and down arrows are switch points of turn on humid N_2 and pure N_2, respectively); (b) The linear relationship between response to humidity and relative humidity at 15 ± 0.3 °C.

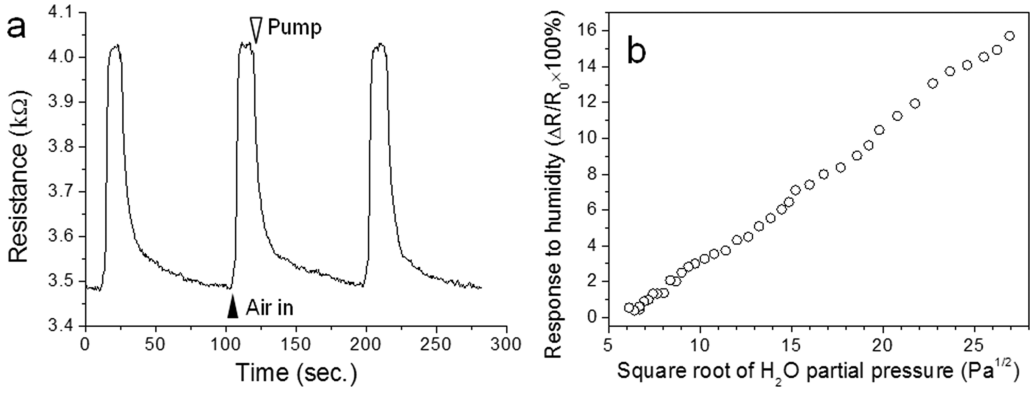

Figure 4. (a) The humidity response of SiC nanopaper by testing of method **II** and (b) response to humidity on the function of square root of H_2O partial pressure (the up and down arrow is the switch point of injecting air and pumping out air, respectively).

change of exposing to analyte. Obviously, the resistance of SiC nanopaper depends on the concentration of water vapor in testing atmosphere. And note that the resistance of SiC nanopaper linearly increases with the increasing RH (Figure 3b). The sensor also shows excellent repeatability of humidity response as shown in Figure S4, which indicates that the highly reversible interactions between water molecules and SiC nanopaper should be dominated by physisorption. Similar to other humidity-sensing materials, SiC nanopaper demonstrates clear humidity hysteresis (Figure S5b). The humidity hysteresis or delay of response intensity may be caused by the capillary condensation effects in the microgaps of SiC nanopaper during the adsorption and desorption process.[6]

$$\text{response to humidity} = (\Delta R/R_0) \times 100\% \quad (1)$$

Lower air pressure means the lower partial pressure of H_2O in the quartz tube. H_2O molecules adsorbed on the SiC nanopaper would desorb in vacuum like other gas molecules. The vacuum process in the quartz tube can reduce the H_2O partial pressure of the testing system, which was named as method **II**. The vacuum degree variation in quartz tube was measured by a vacuometer. As shown in Figure 4a, the resistance of SiC nanopaper decreases with increasing vacuum degree and shows good reproducibility. According to eq 1, the response to humidity is ~16.4% in air (37% RH). When H_2O molecules adsorbed on the surface of SiC nanopaper, the effective carrier density of SiC nanopaper might be proportional to the fraction (θ) of the surface covered by water molecules, which lead to linear resistance increment of SiC nanopaper with increasing RH. Thus, the resistance variation (response to humidity defined in eq 1) should be proportional to θ of the surface that is covered by H_2O molecules ($\theta \ll 1$). The relationship between pressure and resistance could be obtained by combination of pressure−time and resistance−time curves. Figure 4b is the calculated curve of response to humidity versus square root of H_2O partial pressure. The linear correlation between the response to humidity and square root of H_2O partial pressure could be understood with the Langmuir adsorption isotherm theory.[29] According to the monomolecular layer adsorption theory of dissociated gas, the adsorption rate is $r_a = k_a p(1 - \theta)^2$, while the desorption rate is $r_d = k_d\theta^2$ if one decomposed gas molecule occupies two adsorption sites (centers). The k_a and k_d in above equations is the adsorption and desorption constant, respectively. p and θ represent the gas partial pressure and the fraction of the surface adsorbed by gas molecules, respectively. When r_a equals r_d, we can get

$$\theta/(1 - \theta) = (k_a/k_d)^{1/2} p^{1/2} \quad (2)$$

The equation indicates that θ is proportional to $p^{1/2}$ at lower gas coverage ($\theta \ll 1$). Considering H_2O molecules adsorbed on SiC nanopaper are dominated by physisorption and hard to decompose, the phenomenon that one molecule occupies two adsorption sites (centers) may be attributed to one H_2O molecule forming two hydrogen bonds on the surface of SiC nanowires. The good linearity of the correlation between the response to humidity of SiC nanopaper and square root of H_2O

partial pressure indicates a single-layer adsorption mechanism in low RH atmosphere (37% RH to 4% RH or 0.6% to 160 ppm at 15 ± 0.3 °C).

The response/recovery time of SiC nanopaper is usually defined as reaching 90% and 10% of maximum sensitivity. Relatively fast response and recovery time of method **I** is ∼41/124 s, while those of method **II** are 4.5/25.9 s. Because the airtight chamber, which conducts the humidity performance test of SiC nanopaper (testing chamber), was filled with dry N_2 before injecting humid N_2, it is reasonable that the humidity of the testing chamber is gradually changing with continuously introducing of humid N_2 (method **I**). On the other hand, SiC nanopaper is very sensitive to humidity variation. Thus, for method **I**, it needs longer time to change the RH in the testing chamber compared with the method **II** (a rotary mechanical pump was used to expel air from testing chamber). Without changing SiC nanopaper, the difference of the response time within the above two experiments should be attributed to the different rate of RH change in methods **I** and **II**. Obviously, the delay time of changing RH in testing chamber is longer than the response time of SiC nanopaper in method **I**. And the results indicate the SiC nanopaper could make a quick response to the humid change in method **II**. Therefore, we have a further question whether the response time will further shorten or not if faster-changing RH is applied.

Figure S3III presents a lab-made equipment named as "pulsed N_2 flow humidity-sensor testing system" to determine the response time of SiC nanopaper in air. The pulsed high-purity N_2 flow was used to inject humidity to SiC nanopaper sensor at 15 ± 0.3 °C. A mass-flow controller was applied to control the N_2 flow with a pulse time of 0.5 s. As shown in Figure 5, the resistance of SiC nanopaper is dramatically

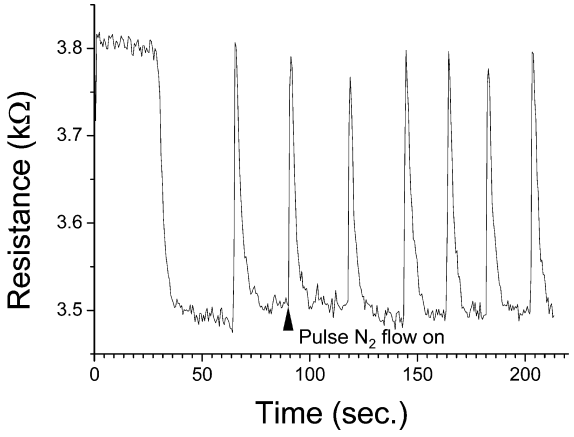

Figure 5. Humidity response of SiC nanopaper in pulse N_2 flow (up arrow is the point of ejecting humid N_2 to SiC nanopaper).

increased and repeatedly reached the maximum zone when the system turned on. As to the definition of response/recovery time mentioned above, 0.8 s and 5.6 s—a very short average response and recovery time of SiC nanopaper was obtained. To our best knowledge, it is the shortest humidity response time compared to many humidity sensors (Table 1). Such a short response time could be attributed to the fast carrier transfer between SiC nanopaper and water molecules and the fast change of RH in the small area above the SiC nanopaper within a very short time.

The humidity-sensing properties of SiC nanopaper treated in acid, alkali, and oxidization air was also tested. After refluxing in concentrated HNO_3, HCl, and NaOH for 30 min, respectively, the three samples of SiC nanopaper did not show an apparent deterioration of humidity-sensing performance. However, high-temperature oxidation could lead to deterioration of humidity-sensing performance of SiC nanopaper. Among the SiC nanopaper oxidized at 600, 750, and 900 °C, SiC nanopaper shows poor humidity-sensing property when the oxidation time exceeded 15 min and temperature was higher than 750 °C (Figure S8). On the basis of TEM observations, it can be seen that the humidity-sensing performance of SiC nanopaper decreases significantly when the thickness of oxide layer is more than 3.4 nm (Figures S6 and S7). The thicker oxide layer may cause a significant interference in the adsorption of water vapor and the carrier transfer from SiC nanowire to external circuit.

Table 1. Response Time of Humidity Sensors Based on Nanomaterials

sensing materials	response time (s) of reaching *x*% of max sensitivity		device type	ref.
ZnO nanotetrapods	36	95%	resistive	1
single SnO_2 nanowires	120−170	90%	resistive	2
ZnO nanowires/rods	3	100%	resistive	7
CeO_2 nanowires	3		resistive	8
TiO_2 nanofibers	∼3	100%	resistive	30
$Na_3Ti_3O_7$ nanowires	4	100%	resistive	9
graphene quantum dots	∼20		resistive	5
SiC nanopaper	∼0.8	90%	resistive	this work
Al_2O_3 nanotubes	10	90%	capacitive	6
MWCNTs	16	100%	capacitive	31
SiC nanowires	105	90%	capacitive	32

The surface chemical conditions of SiC nanopaper is closely related to the humidity-sensing properties. However, as the building blocks of SiC nanopaper, the as-prepared centimeters-long SiC nanowires have thin amorphous sheath[25] of an average thickness of 1.1 nm (Figure S6a). To clarify the chemical composition and structure of the thin layer is important to understand the humidity-sensing properties of SiC nanopaper. A powerful method, the XPS depth profile, was applied to analyze the surface chemical composition in the range of several nanometers. Figure 6a shows the surveys of SiC nanowires of etching times of 0, 20, 100, 180, 260, 340, 420, and 540 s, respectively. Oxygen, nitrogen, silicon, and carbon were found in the surface (Figure 6b), but the signals of nitrogen and oxygen decreased during the etching treatment. The oxygen peaks (O 1s peaks in Figure 6a,d) clearly demonstrate the oxygen content dramatically decreased from 20.14 to 4.31 atom % within the first 100 s of etching. According to the results of peak-fitting analysis, the percent of Si−N and Si−O bonds were gradually reduced in the surface of SiC nanowires, while the Si−C bond was rapidly increasing and reaching a nearly steady state after 100 s of etching (Figure 6c). The total amount of Si atoms that covalently bonded with oxygen (∼103.3 eV) was ∼17 atom %, while the amount of oxygen atom is 20.14 atom %, which means the oxide layer is not stoichiometry SiO_2. Furthermore, the adsorbed H_2O or O_2 molecules, especially the chemisorbed ones, are hardly detached completely by etching treatment. Therefore, the bonding energy within the range of 531.3−532.7 eV (shadow area in Figure 6d) can be attributed to the chemisorbed H_2O or O_2[33−35] due to surface hydroxyl.[36]

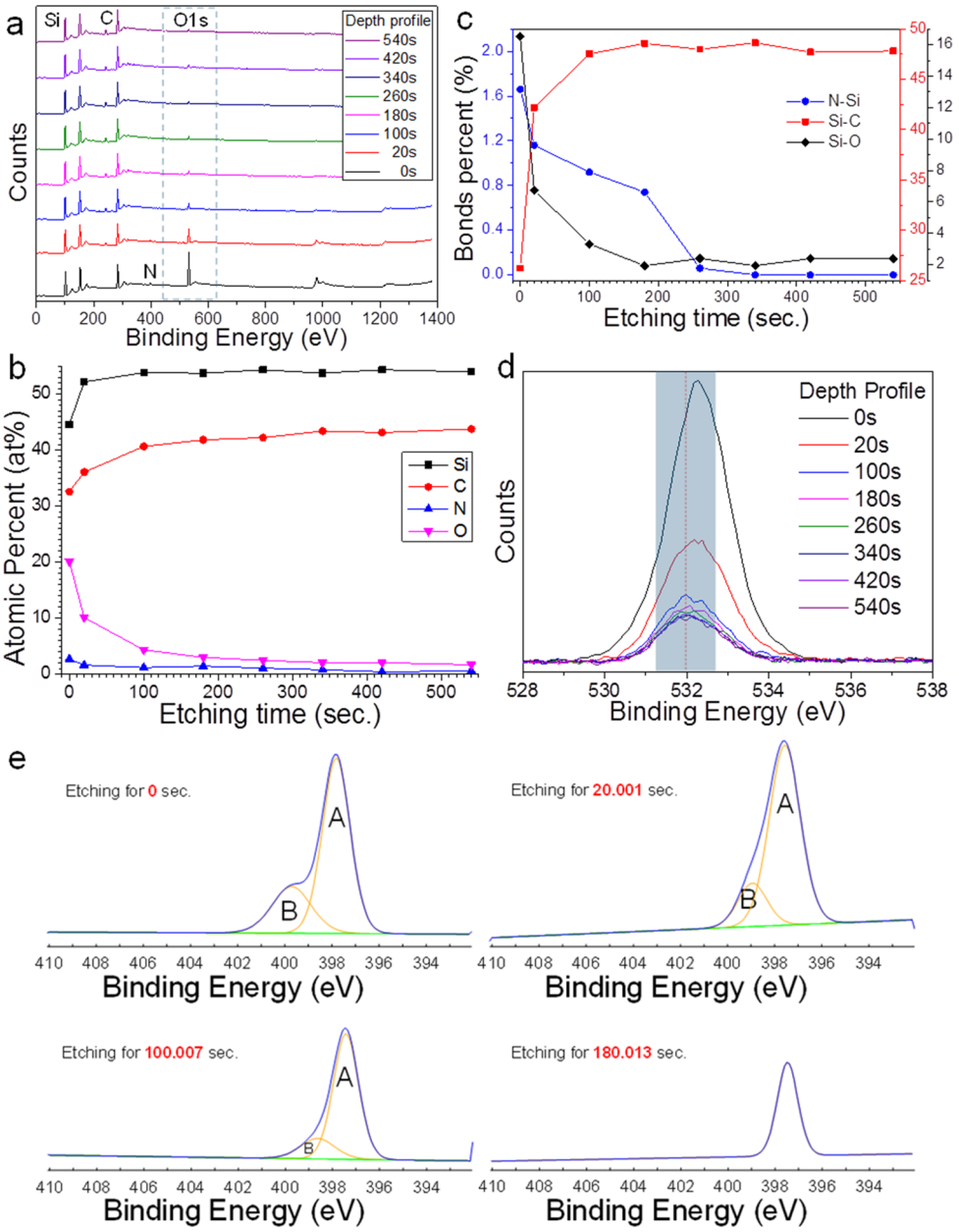

Figure 6. Depth profile analysis of SiC nanowires at etching time of 0, 20, 100, 180, 260, 340, 420, and 540 s, respectively. (a) surveys of SiC nanowires; (b) the variation of element contents in the surface of SiC nanowires during the etching treatment; (c) bonds percent analysis of the surface of SiC nanowires according to peaks fitting results; (d) high-resolution XPS spectra of the oxygen in the surface of SiC nanowires; (e) high-resolution XPS spectra of nitrogen in the surface of SiC nanowires at etching times of 0, 20, 100, and 180 s, respectively; the A and B represent the peaks centered at 397.7 and 399.3 eV.

High-resolution analysis of nitrogen in the surface of SiC nanowires (Figure 6e) indicated that most nitrogen atoms are bonded with silicon (named as peak A and centered at 397.7), and a few bonded with carbon (named as peak B and 399.3 eV). The peak A and B gradually decreased during the etching treatment, but peak B disappeared after etching for 180 s. The signal of peak A did not vanish even after etching treatment for 540 s (nitrogen content is 0.54 atom %). The same phenomenon (Figure 6d) appeared again in the depth profile of oxygen after 540 s of etching treatment (oxygen content is 1.61 atom %). Considering the practical experimental facts of XPS depth profile analysis, it is inevitable to detect some weak signals from the area behind the actual surface, especially for powder samples and samples like SiC nanowires.

As reported in many papers, formation of the silicon oxide sheath can be attributed to the residual oxygen in the atmosphere during the growth of SiC nanowires. And the surface of silicon oxide was covered with a large number of silanol groups[36] that could easily form hydrogen bond with water molecules. Researchers have found that the water layer formed on silicon oxide at RH lower than 30% is a completely hydrogen-bonded icelike network, and that liquid water layer will form at higher RH.[37] These research results can indirectly support the result from XPS depth profile of SiC nanowires. According to the XPS analysis, the chemical composition of the amorphous layer on SiC nanowires (Figure S6a) is silicon oxide-based SiCNO amorphous sheath with silanol groups.

dx.doi.org/10.1021/am5067496 | ACS Appl. Mater. Interfaces 2014, 6, 22673−22679

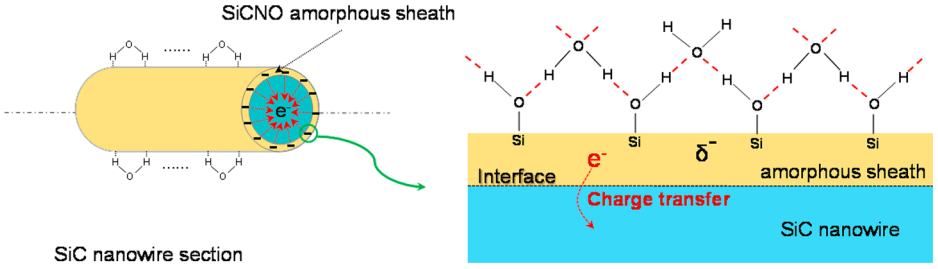

Figure 7. Proposed humidity-sensing mechanism of SiC nanopaper.

Experiments[4] and theoretical calculations[3] have confirmed that the hydrogen bonds formed on the surface of CNT can lead to electron transfer between water layer and CNT. Considering hydrogen bonds likely formed in SiC nanopaper, which probably leads to charge transfer, the sensing mechanism of SiC nanopaper could be interpreted as Figure 7.

In the sensing process, hydrogen bond forms between H_2O and SiCNO amorphous sheath as soon as water molecule is adsorbed on the sheath of SiC nanopaper. As shown in Figure 7, the dangling silanol groups of SiC nanopaper are active sites to form hydrogen bonds between water molecules and the sheath. The formation of the hydrogen bonds leads to a slightly negative charge of the sheath, since water molecules donate electrons.[4] Then the electrons in the sheath and water molecules layer are transferred to the inner SiC nanowires for charge balance. The electron transfer will reduce the effective carrier density of the p-type SiC nanowires and thus leads to the increment of resistance of SiC nanopaper.

CONCLUSIONS

In summary, a simple method was developed for preparing free-standing SiC nanopaper. The resistance of SiC nanopaper linearly increases with increasing environment RH within very short response time (the fastest is 0.8 s), which indicates that this new paperlike material is highly sensitive to water vapor. As a p-type semiconductor, the intriguing humidity-sensing performance is probably attributed to the decrement of effective carrier density of SiC nanopaper aroused by reversible physisorption of water molecules, which could be interpreted as electron transfer from water molecules to SiC nanopaper. As new material with excellent humidity-sensing property, SiC nanopaper might easily find applications in high-performance gas sensors after proper chemical modifications. And the simple method of fabricating devices that have advantages including low cost and ease of processing and scale-up could be widely applied in other paperlike nanomaterials without relying on any microfabrication techniques.

METHODS

Preparation of Centimeters-Long SiC Nanowires. The preparation and characterization of centimeters-long SiC nanowires has been reported elsewhere.[25] In a typical procedure, polysilacarbosilane (4.0 g) and ferrocene (0.04 g) were introduced into active carbon (5.0 g) to form homogeneous slurry, which is placed in a ceramic boat and pushed to the center of a tube furnace with another two empty ceramic boats. The system was heated to 1300 °C at 10 °C/min in highly pure N_2 atmosphere and maintained at 1300 °C for 3 h. Then the cotton-like centimeters-long SiC nanowires were found covering on the empty ceramic boats after the furnace cooled to room temperature.

Fabrication of SiC Nanopaper and SiC Nanopaper Humidity Sensor. Cotton-like centimeters-long SiC nanowires were first placed on smooth substrates that SiC nanopaper could be easily peeled off. Then several drops of acetone were dropped on the cotton-like nanowires and allowed to volatilize naturally at room temperature. The cotton-like centimeters-long SiC nanowires were compressed to a piece of SiC nanopaper during the process. SiC nanopaper could be tailored if using weighing paper as substrate. Photos of tailoring SiC nanopaper are available in Supporting Information (see Figure S1).

A piece of SiC nanopaper was placed on a slightly bigger silicon wafer, and then Au electrode was sputtering on the wafer with an alumina foil (1.5 mm in width). The sputtering current was ~10 mA during the sputtering process, while the vacuum degree was lower than 10 Pa.

Characterization of Humidity-Sensing Performance of SiC Nanopaper. Special designed systems are applied to measure the resistance variety of SiC nanopaper humidity sensor in humid nitrogen atmosphere with different relative humidity. Three systems (**I**, **II**, and **III**) are applied to change the RH of testing system (see the schematic illustrations of testing systems shown in Figure S3).

I: The humidity testing system is illustrated in Figure S3 I, humid environment of different RH is obtained by controlling the flow rate of highly pure nitrogen and humid nitrogen through two mass flow controllers marked as MFC1 and MFC2. A commercial hygrometer was employed to determine the RH of testing environment. The resistance variation of SiC nanopaper is measured by digital multimeter (Agilent 34411A).

II: The partial pressure of H_2O decreases with decreasing air pressure. So as another way to change the water molecule concentration of testing atmosphere, a mechanical pump is applied to pump out air of quartz tube when the two MFC turned off (as in Figure S3 II). The system could be pumped to vacuum and released to air repeatedly. During the period, resistance change of SiC nanopaper and pressure variation of testing atmosphere could be measured by digital multimeter and vacuometer simultaneously.

III: As shown in Figure S3 III, a lab-made pulse airflow humidity sensor testing system is used to test the sensing properties of SiC nanopaper. This simple device could quickly change the RH of a small area above SiC nanopaper in air for a fast and microscale detection.

ASSOCIATED CONTENT

Supporting Information

Detailed information on preparation and characterization of centimeters-long SiC nanowires, including photos, SEM and TEM images, as well as XRD analysis; tailoring photos of SiC nanowires, schematic illustrations of humidity testing system of SiC nanopaper, TEM analysis of oxidation of SiC nanopaper, and the humidity-sensing performance of SiC nanopaper oxidized at 750 °C for 30 min. This material is available free of charge via the Internet at http://pubs.acs.org.

AUTHOR INFORMATION

Corresponding Author

*E-mail: nudtlgy@163.com.

Notes

The authors declare no competing financial interest.

■ ACKNOWLEDGMENTS

The authors are thankful for the help from Mr. Y. Yang, as well as the financial support from the National Natural Science Foundation of China (Grant Nos. 51102281 and 11104348) and Research Project of National University of Defense Technology (Grant No. JC13-02-11).

■ REFERENCES

(1) Qiu, Y.; Yang, S. ZnO Nanotetrapods: Controlled Vapor-Phase Synthesis and Application for Humidity Sensing. *Adv. Funct. Mater.* **2007**, *17*, 1345−1352.
(2) Kuang, Q.; Lao, C.; Wang, Z. L.; Xie, Z.; Zheng, L. High-Sensitivity Humidity Sensor Based on a Single SnO_2 Nanowire. *J. Am. Chem. Soc.* **2007**, *129*, 6070−6071.
(3) Pati, R.; Zhang, Y.; Nayak, S. K.; Ajayan, P. M. Effect of H_2O Adsorption on Electron Transport in a Carbon Nanotube. *Appl. Phys. Lett.* **2002**, *81*, 2638−2640.
(4) Zahab, A.; Spina, L.; Poncharal, P.; Marlière, C. Water-Vapor Effect on the Electrical Conductivity of a Single-Walled Carbon Nanotube Mat. *Phys. Rev. B* **2000**, *62*, 10000−10003.
(5) Sreeprasad, T. S.; Rodriguez, A. A.; Colston, J.; Graham, A.; Shishkin, E.; Pallem, V.; Berry, V. Electron-Tunneling Modulation in Percolating Network of Graphene Quantum Dots: Fabrication, Phenomenological Understanding, and Humidity/Pressure Sensing Applications. *Nano Lett.* **2013**, *13*, 1757−1763.
(6) Cheng, B.; Tian, B.; Xie, C.; Xiao, Y.; Lei, S. Highly Sensitive Humidity Sensor Based On Amorphous Al_2O_3 Nanotubes. *J. Mater. Chem.* **2011**, *21*, 1907−1912.
(7) Zhang, Y.; Yu, K.; Jiang, D.; Zhu, Z.; Geng, H.; Luo, L. Zinc Oxide Nanorod and Nanowire for Humidity Sensor. *Appl. Surf. Sci.* **2005**, *242*, 212−217.
(8) Fu, X. Q.; Wang, C.; Yu, H. C.; Wang, Y. G.; Wang, T. H. Fast Humidity Sensors Based On CeO_2 Nanowires. *Nanotechnology* **2007**, *18*, 145503.
(9) Zhang, Y.; Fu, W.; Yang, H.; Li, M.; Li, Y.; Zhao, W.; Sun, P.; Yuan, M.; Ma, D.; Liu, B.; Zou, G. A Novel Humidity Sensor Based On $Na_2Ti_3O_7$ Nanowires with Rapid Response-Recovery. *Sens. Actuators, B* **2008**, *135*, 317−321.
(10) Yeow, J. T. W.; She, J. P. M. Carbon Nanotube-Enhanced Capillary Condensation for a Capacitive Humidity Sensor. *Nanotechnology* **2006**, *17*, 5441−5448.
(11) Mclaughlin, S. B.; Taylor, G. E. Relative Humidity: Important Modifier of Pollutant Uptake by Plants. *Science* **1981**, *211*, 167−169.
(12) Willett, K. M.; Gillett, N. P.; Jones, P. D.; Thorne, P. W. Attribution of Observed Surface Humidity Changes to Human Influence. *Nature* **2007**, *449*, 710−713.
(13) Kim, H.; Haensch, A.; Kim, I.; Barsan, N.; Weimar, U.; Lee, J. The Role of NiO Doping in Reducing the Impact of Humidity on the Performance of SnO_2-Based Gas Sensors: Synthesis Strategies, and Phenomenological and Spectroscopic Studies. *Adv. Funct. Mater.* **2011**, *21*, 4456−4463.
(14) Liu, J.; Rinzler, A. G.; Dai, H.; Hafner, J. H.; Bradley, R. K.; Boul, P. J.; Lu, A.; Iverson, T.; Shelimov, K.; Huffman, C. B.; Rodriguez-Macias, F.; Shon, Y.; Lee, T. R.; Colbert, D. T.; Smalley, R. E. Fullerene Pipes. *Science* **1998**, *280*, 1253−1256.
(15) Bahr, J. L.; Yang, J.; Kosynkin, D. V.; Bronikowski, M. J.; Smalley, R. E.; Tour, J. M. Functionalization of Carbon Nanotubes by Electrochemical Reduction of Aryl Diazonium Salts: A Bucky Paper Electrode. *J. Am. Chem. Soc.* **2001**, *123*, 6536−6542.
(16) Vigolo, B.; Nicaud, A. P.; Coulon, C.; Sauder, C. D.; Pailler, R.; Journet, C.; Bernier, P.; Poulin, P. Macroscopic Fibers and Ribbons of Oriented Carbon Nanotubes. *Science* **2000**, *290*, 1331−1334.
(17) Zhang, L.; Zhang, G.; Liu, C.; Fan, S. High-Density Carbon Nanotube Buckypapers with Superior Transport and Mechanical Properties. *Nano Lett.* **2012**, *12*, 4848−4852.
(18) Chen, H.; Müller, M. B.; Gilmore, K. J.; Wallace, G. G.; Li, D. Mechanically Strong, Electrically Conductive, and Biocompatible Graphene Paper. *Adv. Mater.* **2008**, *20*, 3557−3561.
(19) Dikin, D. A.; Stankovich, S.; Zimney, E. J.; Piner, R. D.; Dommett, G. H. B.; Evmenenko, G.; Nguyen, S. T.; Ruoff, R. S. Preparation and Characterization of Graphene Oxide Paper. *Nature* **2007**, *448*, 457−460.
(20) Ballard, D. G. H.; Rideal, G. R. Flexible Inorganic Films and Coatings. *J. Mater. Sci.* **1983**, *18*, 545−561.
(21) Hu, L.; Choi, J. W.; Yang, Y.; Jeong, S.; La Mantia, F.; Cui, L.; Cui, Y. Highly Conductive Paper for Energy-Storage Devices. *Proc. Natl. Acad. Sci. U.S.A.* **2009**, *106*, 21490−21494.
(22) Wang, D.; Li, F.; Zhao, J.; Ren, W.; Chen, Z.; Tan, J.; Wu, Z.; Gentle, I.; Lu, G. Q.; Cheng, A. H. Fabrication of Graphene/Polyaniline Composite Paper Via in Situ Anodic Electropolymerization for High-Performance Flexible Electrode. *ASC Nano* **2009**, *3*, 1745−1752.
(23) Mei, Q.; Zhang, Z. Photoluminescent Graphene Oxide Ink to Print Sensors Onto Microporous Membranes for Versatile Visualization Bioassays. *Angew. Chem., Int. Ed.* **2012**, *51*, 5602−5606.
(24) Harris, G. L. *Properties of Silicon Carbide;* INSPEC, the Institution of Electrical Enginneers: London, U.K., 1995; p 282.
(25) Li, G. Y.; Li, X. D.; Chen, Z. D.; Wang, J.; Wang, H.; Che, R. C. Large Areas of Centimeters-Long SiC Nanowires Synthesized by Pyrolysis of a Polymer Precursor by a CVD Route. *J. Phys. Chem. C* **2009**, *113*, 17655−17660.
(26) Chen, Y.; Zhang, X.; Zhao, Q.; He, L.; Huang, C.; Xie, Z. *P*-type 3C-SiC Nanowires and their Optical and Electrical Transport Properties. *Chem. Commun.* **2011**, *47*, 6398−6400.
(27) Seong, H. K.; Choi, H. J.; Lee, S. K.; Lee, J. I.; Choi, D. J. Optical and Electrical Transport Properties in Silicon Carbide Nanowires. *Appl. Phys. Lett.* **2004**, *85*, 1256−1258.
(28) Zhou, W. M.; Xuan, L.; Zhang, Y. F. Simple Approach to β-SiC Nanowires: Synthesis, Optical, and Electrical Properties. *Appl. Phys. Lett.* **2006**, *89*, 223124.
(29) Laidler, K. J. *Chemical Kinetics;* McGraw-Hill: New York, 1965; p 260.
(30) Li, Z.; Zhang, H.; Zheng, W.; Wang, W.; Huang, H.; Wang, C.; MacDiarmid, A. G.; Wei, Y. Highly Sensitive and Stable Humidity Nanosensors Based On LiCl Doped TiO_2 Electrospun Nanofibers. *J. Am. Chem. Soc.* **2008**, *130*, 5036−5037.
(31) Zhao, Z.; Liu, X.; Chena, W.; Li, T. Carbon Nanotubes Humidity Sensor Based On High Testing Frequencies. *Sens. Actuators, A* **2011**, *168*, 10−13.
(32) Wanga, H. Y.; Wang, Y. Q.; Hu, Q. F.; Li, X. J. Capacitive Humidity Sensing Properties of Sic Nanowires Grown On Silicon Nanoporous Pillar Array. *Sens. Actuators, B* **2012**, *166−167*, 451−456.
(33) Wei, D.; Liu, Y.; Wang, Y.; Zhang, H.; Huang, L.; Yu, G. Synthesis of N-Doped Graphene by Chemical Vapor Deposition and its Electrical Properties. *Nano Lett.* **2009**, *9*, 1752−1758.
(34) Fu, L.; Liu, Z.; Liu, Y.; Han, B.; Hu, P.; Cao, L.; Zhu, D. Beaded Cobalt Oxide Nanoparticles Along Carbon Nanotubes: Towards More Highly Integrated Electronic Devices. *Adv. Mater.* **2005**, *17*, 217−221.
(35) Wang, X.; Liu, Y.; Zhu, D.; Zhang, L.; Ma, H.; Yao, N.; Zhang, B. Controllable Growth, Structure, and Low Field Emission of Well-Aligned CN_x Nanotubes. *J. Phys. Chem. B* **2002**, *106*, 2186−2190.
(36) Iler, P. K. *The Chemistry of Silica;* Wiley: New York, 1970.
(37) Asay, D. B.; Kim, S. H. Evolution of the Adsorbed Water Layer Structure On Silicon Oxide at Room Temperature. *J. Phys. Chem. B* **2005**, *109*, 16760−16763.